

## Article

# Wear and the Transition from Static to Mixed Lubricated Friction of Sorption or Spreading Dominated Metal-Thermoplastic Contacts

Christof Koplin <sup>1,\*</sup> , Harald Oehler <sup>2</sup>, Olaf Praß <sup>2</sup>, Bernadette Schlüter <sup>1</sup>, Ingo Alig <sup>2</sup>  and Raimund Jaeger <sup>1</sup>

<sup>1</sup> Fraunhofer IWM MikroTribologie Centrum, Wöhlerstr. 9, 79108 Freiburg, Germany; bernadette.schlueter@iwm.fraunhofer.de (B.S.); raimund.jaeger@iwm.fraunhofer.de (R.J.)

<sup>2</sup> Fraunhofer LBF, Bereich Kunststoffe, Schlossgartenstraße 6, 64289 Darmstadt, Germany; harald.oehler@lbf.fraunhofer.de (H.O.); olafprass@web.de (O.P.); ingo.alig@lbf.fraunhofer.de (I.A.)

\* Correspondence: christof.koplin@iwm.fraunhofer.de; Tel.: +49-761-5142-269

**Abstract:** Stiction, run-in wear and friction of lubricated polyoxymethylene homopolymer (POM)- and aliphatic polyamide (PA46)-steel tribosystems were investigated for mild-loaded mixed lubrication conditions with and without thermal conditioning of the polymers in the lubricant prior to testing. Macroscopic oscillatory tribometry and standard gliding experiments were carried out. The hypothesis that sorption of a lubricant into a thermoplastic polymer and partial solving of the surface by the lubricant can change wear rate and friction was tested. It was found that for POM-lubricant-pairings, the tribological behavior is dominated by the sorption of the lubricant into the polymer; it is not influenced by the spreading energy. For the PA46-lubricant pairings, no mass uptake by sorption was measured, and the tribological behavior is influenced by spreading and changes in hardness due to thermal aging. For mild loading in mixed lubricated conditions, friction and wear properties seem to be primarily determined by the hardness-dependence of abrasive contact and less by adhesion or hysteretic mechanisms.



**Citation:** Koplin, C.; Oehler, H.; Praß, O.; Schlüter, B.; Alig, I.; Jaeger, R. Wear and the Transition from Static to Mixed Lubricated Friction of Sorption or Spreading Dominated Metal-Thermoplastic Contacts. *Lubricants* **2022**, *10*, 93. <https://doi.org/10.3390/lubricants10050093>

Received: 8 April 2022

Accepted: 9 May 2022

Published: 12 May 2022

**Publisher's Note:** MDPI stays neutral with regard to jurisdictional claims in published maps and institutional affiliations.



**Copyright:** © 2022 by the authors. Licensee MDPI, Basel, Switzerland. This article is an open access article distributed under the terms and conditions of the Creative Commons Attribution (CC BY) license (<https://creativecommons.org/licenses/by/4.0/>).

**Keywords:** spreading; sorption; plasticization; mixed-lubrication; wear; polymer; run-in; stiction; surface hardness

## 1. Introduction

Tribologically loaded components, which are used in mechanical engineering or in the automotive industry, can be made from thermoplastic polymers. As a result, one obtains lightweight and energy-efficient products or components, which exhibit superior performance with respect to noise, vibration and harshness. The use of polymers in tribological applications requires a profound understanding of the friction and wear behavior of polymers [1]. In particular, the tribology of lubricated polymer-steel contacts is complex and remains an area of active research. The complexity partially arises from the interaction of the polymer, lubricant, and the steel frictional partner. The observation of polymer transfer [2] and the “temperature hot spots” [3] of the polymer during frictional loading in lubricated systems indicates that adhesive friction contributes to the tribology of polymers. Furthermore, physico-chemical interactions between the frictional partners, such as sorption of the lubricant in the polymer and vice versa, have to be considered.

In previous studies [4,5], the transition from static to dynamic boundary friction of lubricated poly(ether etherketone) (PEEK)- and poly(amide) 46 (PA46)-steel-contacts was investigated with oscillatory tribometry. The differences in the tribological behavior for different ester-based lubricants, pentaerythrite ester (PEEs) and trimellitic acid ester (TAEs) and poly(1-decene) as non-polar lubricants, on the one hand, and water, glycerine, and ethylene glycol as polar lubricants on the other hand were explained by differences in the surface and interfacial energies. All investigated polymer-lubricant pairings show that the

coefficient of friction at low gliding velocities and the spreading energy are closely related, where  $W_{spreading}$  describes the tendency of the lubricant to enter the tribological contact. The pairings where the lubricant has a higher tendency to spread into the tribological contact exhibit a lower coefficient of friction at very low gliding speeds. For PA46, indications for partial sorption of polar lubricants at the polymer surface and/or partial solving of the polymer by the lubricant were found to influence friction.

In this paper, sorptive POM-lubricant-pairings were studied to investigate the influence of sorption and swelling of the thermoplastic matrix and the resulting plasticization on the tribological properties. The material properties and the tribological parameters are correlated to physico-chemical parameters such as the sorption, the surface tension and the Hildebrand parameters as well as the parameters  $W_{solving}$  and  $W_{spreading}$ , which were used in the previous studies. For the sorptive pairings, the solving energy ( $W_{solving}$ ) can be considered to be a measure for both the sorption of the lubricant within the polymer and (to a less extent) solving of the polymer by the lubricant since both mechanisms are based on similar molecular interactions between the polymer and the organic liquid. Thus, the influence of the spreading and solving tendency on the adhesion threshold as well as the sorption-driven mechanisms were tested at room temperature for semicrystalline non-polar POM with a rubber-like amorphous phase with non-polar base oils. POM is expected to be soluble in polar lubricants. Non-sorptive PA46-oil pairings are included in the study as a comparison. Here, the tribological properties are also correlated to  $W_{solving}$  and  $W_{spreading}$  but without plasticization effects due to swelling of the polymer matrix by the lubricants. In contrast to those lubricants, PA46 paired with water or ethyleneglycole shows significant sorption and plasticization by wakening the hydrogen bonds of polyamide.

Consequently, the concept of the tendency of lubricants for thermoplastic polymers to dissolve and spread has been extended to sorptive polymer-lubricant pairings. Bormuth et al. [6] found circumstantial evidence of a reduction in mechanical characteristics due to viscoelastic and viscoplastic effects after aging of POM in lubricants. They found an increased stiction and decreased hardness after storage in the lubricant that was explained by increased adhesive sticking due to a larger real contact area by creep. In this view, the solving/sorption tendency measured by  $W_{solving}$  should indicate interactive mechanisms beyond the physical motivation of the interfacial energy  $\gamma_{13}$  and indicate the impact of sorption of oils in the polymer and solving of polymer into the oil. If there is an indication for an increased polymer-lubricant interaction, the impact on near-surface properties should be measurable. Either adhesive, viscoelastic or viscoplastic properties near the surface are the essential factors for the wear behavior of rough lubricated contacts. Furthermore, thermal aging effects due to chemical degradation of the polymer chains and/or changes in the semicrystalline structure during storage in the lubricants or nitrogen atmosphere were considered.

The following hypotheses were formulated:

- (A) A low but relevant solving tendency can be found for the sorptive and swelling thermoplastic (POM) systems in semicrystalline polymers (here: lubricants in POM).
- (B) Sorption of lubricants results in a decrease in hardness and shear modulus by plasticization of the polymer matrix and is related to the solving energy or corresponding solubility parameters of the actual polymer-lubricant pairing. This seems to be justified by the similar polymer-lubricant interactions in the case of a solution of a polymer in a solvent and for sorption of the solvent in the polymer.
- (C) Run-in wear rate and run-in friction depend on  
the adhesion threshold, measured by stiction,  
the mechanical properties of the polymers due to abrasive interaction, and  
the viscoelastic properties and hysteretic deformation.
- (D) A low solving system (from  $0 < 5$  mN/m, as for POM in oils) leads to more pronounced increased stiction by an increase in chain mobility, in comparison to high solving systems (PA46 in water, ethyleneglycole or glycerine) that showed a smeared-out transition to gliding.

- (E) Sorptive pairings with low solving energy are not sensitive to spreading due to dominant interactive mechanisms.

To speed up high non-polar–non-polar interaction, low-viscosity base oils were used. The hypotheses for an impact of the interaction energies on interfacial mechanisms on the adhesion threshold will be extended to hypotheses for an impact on cohesive mechanisms on the run-in wear and friction behavior at mixed lubricated gliding.

## 2. Motivation and Scientific Background

The experimental studies discussed in the current paper focus on the effect of lubricants on the gliding contact of semicrystalline thermoplastic materials and a rough frictional partner with higher hardness and good thermal conductivity. For these systems, the main tribological mechanisms are usually expected to be interfacial and cohesive interactions [7] that can be described mainly by adhesion [8] or plowing [9].

The adhesive friction of polymers arises from the continuous forming and breaking of adhesive bonds between the two gliding partners. This process was described by Schallamach [8] as a thermally driven rate process. Schallamach's model was confirmed experimentally in a range of studies [10–12] and refined by, e.g., Singh et al. [13]. In a recent paper by Sinha et al. [14], adhesive friction of a gelatin hydrogel was linearly related to Coulomb's law of friction. The hysteretic friction of the amorphous phase of a semicrystalline polymer can be treated similarly to the hysteretic friction of elastomers and correlates with the loss modulus [15]. A good correlation to friction was found for the wetting and spreading parameters of lubricated self-pairing contacts for a wide range of lubricants [16,17].

Quantities such as the work of spreading  $W_{spreading}$  (2) and the work of solving  $W_{solving}$  (3) can be determined from surface- and interfacial energies. The determination of surface and interfacial energies (1) of the frictional partners  $W_{ij}$  is typically based on contact angle measurements ( $i = 1$  refers to the polymer,  $i = 2$  to the steel frictional partner and  $i = 3$  to the lubricant). The ratio of interfacial energy  $\gamma_{13}$  determined by Owen's approach and by a contact angle measurement with the pairing of lubricant and polymer (denoted as  $W_{solving}$ ) is denoted "interaction parameter".

According to [18], polymers are permeable to fluids; however, the extent of permeation depends strongly on the nature of the polymer and the fluid. The transport of liquids in polymers is caused by either a concentration, vapor pressure and/or temperature gradient or, alternatively, by an external force field.

The prediction of the polymer solubility in solvents can be made by an established "rule of thumb": the closer the solubility parameters of the solute and the solvent are, the more likely the solute can be solved in the given solvent. Using the Hansen solubility parameters (4), an approximate spherical "volume" of solubility with radius  $R$  can be drawn for each solute. Only solvents that have Hansen solubility parameters within this volume are likely to dissolve the polymer in question. The interaction radius  $R$  depends on the type of polymer (solvent: 1, polymer: 2, dispersive forces:  $d$ , polar forces:  $p$ , hydrogen bonding:  $h$ ). The surface and the cohesion energy  $\gamma$  of the polymer or liquid are correlated with the Hansen solubility parameter (5) [19].

If a solvent (here the lubricant) is brought into contact with a polymer (sorber), two mechanisms take place; the first is the uptake of the solvent, which leads to increased weight, and the second is the dissolution of polymer chains (as well additives or low molecular components) in the solvent, leading to a weight reduction in the conditioned polymer. The first process is the sorption of a sorber in a polymer matrix, whereas the second one is the solution of the polymer. Although different, both processes are related to the dispersive and polar interactions as well as hydrogen bonding between the molecules. For diffusive transport and sorption, the structure of the sorber (e.g., semicrystalline superstructure, free volume of the amorphous phase) has to be considered. However, since the solution of a polymer in a solvent and the sorption of a liquid in a polymer have similar molecular origins and are related to similar physical–chemical interactions, the

work of solving  $W_{solving}$ , the interfacial energy  $\gamma_{13}$ , the Hansen solubility parameter, or the interaction radius  $R$  can also be used as (approximate) measures for the ability of sorption within the polymer matrix.

Table 1 summarizes the relevant mathematical expressions, and the model parameters are described near the references to the equation.

**Table 1.** Table of equations.

| Property  | Equation   |
|---|--|
| Interfacial energy  | $W_{13} = 2 \cdot \sqrt{\gamma_{11}^p \cdot \gamma_{33}^p} + 2 \cdot \sqrt{\gamma_{11}^d \cdot \gamma_{33}^d}$ (1)   |
| Spreading energy of system  | $W_{spreading} = W_{12} + W_{33} - W_{13} - W_{23}$ (2)  |
| Solving energy of lubricated thermoplastic  | $W_{solving} \leq \gamma_{13} = 1/2W_{11} + 1/2W_{33} - W_{13}$ (3)  |
| Hansen solubility parameters in comparison to interaction radius R                | $\left[4(\delta_{d2} - \delta_{d1})^2 + (\delta_{p2} - \delta_{p1})^2 + (\delta_{h2} - \delta_{h1})^2\right] \leq R^2$ (4)                                   |
| Correlation of surface and the cohesion energy to the Hansen solubility parameter | $\gamma = 0.0146 \cdot [2.28\delta_d^2 + \delta_p^2 + \delta_h^2] M_{vol}^{0.2}$ (5)   |
| Minimal isothermal 3-factor model for mixed lubricated friction                   | $\mu \sim \left[\frac{R_a}{h}\right]^m \rightarrow \mu_{crit} \left[\frac{p}{H}\right]^n \left[\frac{R_a}{\frac{h\sigma}{p}}\right]^m$ (6)                   |
| Minimal isothermal 3-factor model for mixed lubricated wear                       | $\frac{\dot{w}}{v} \sim \left[\frac{R_a}{h}\right]^s \rightarrow k_{crit} \left[\frac{p}{H}\right]^r \left[\frac{R_a}{\frac{h\sigma}{p}}\right]^s$ (7)       |
| Time-dependent relative mass uptake of a plate by Fickian diffusion               | $\phi(t) = \phi_{\infty} \times \left(1 - \frac{8}{\pi^2} \sum_{n=1}^{\infty} \frac{1}{(2n+1)^2} \exp\left(\frac{-D(2n+1)^2 \pi^2 t}{l^2}\right)\right)$ (8) |

The discussions in the current paper are based on the measured mass uptake (8) by sorption of lubricant, the coefficient of friction in boundary lubrication on a polished-like steel surface, the surface hardness of a polymer with an equivalent indentation depth of attacking grinding grooves of the frictional partner and the resulting run-in wear rate and COF in mixed lubrication on a finish ground steel surface. Although time-dependent sorption experiments are performed in this study, for interpretation in the following, only the relative mass uptake after 105 days  $\phi_{105d} = \phi(t = 105d)$  in an isothermal experiment will be used.

The wear of polymers can be explained on a fundamental level as the interaction of cohesive and interfacial wear [7]. The abrasive effect of the frictional partner of the polymer needs to be described on the one hand by the mechanical characteristics of the polymer and on the other hand by the surface topography of the frictional partner. They lead to different “modes of interaction”, i.e., smoothing, plowing or cutting [9,20,21]. Ultimately, the tribological interactions need to be viewed as highly dynamic processes, where, e.g., local heating of the polymer by the frictional power changes the mechanical (specifically the viscoelastic) characteristics of the polymer (up to local melting of the polymer) and the transfer of the polymer to the frictional partner changes the structure and property of the contact partner. Here, one should differentiate between effects that are predominantly due to interfacial interactions of the system and occur only close to the surface (spreading, solving of polymer chains in the lubricant or formation of brushes) and those due to the sorption of the lubricant in the polymer matrix and the related plasticization. Further effects are tribo-chemical reactions in the presence of organic lubricants, which will not be considered in this paper.

Despite the variety of modes of interaction of lubricated polymers, adhesive interaction between the polymer and frictional partner always occurs, either by contact of the polymer with a “smooth” frictional partner, or by the local contact of the polymer with the asperities of a “rough” frictional partner. As a result, studies of the adhesive friction of lubricated polymers with “smooth” surfaces can potentially yield some insight into some aspects of the friction of lubricated polymers with rough surfaces. The local contact area of the polymer with an asperity in boundary lubrication should be higher for a material with a higher equivalent indentation depth. Furthermore, the indentation depth should be higher for a polymer swollen with lubricant. One has to keep in mind that at higher velocities in the mixed lubrication regime, the contact area of the polymer and hard partner is gradually reduced to a few asperities when the transition to hydrodynamic friction occurs. The chosen minimal isothermal 3-factor model for mixed lubricated friction  $\mu$  (6) and wear coefficient  $k$  (7) factorizes the transition behavior in mixed lubrication with respect to effective roughness  $R_a$  and the mechanical interaction intensity with respect to surface hardness  $H$ . The system and loading parameters  $p$ : pressure,  $v$ : velocity,  $h$ : viscosity were used as well as the remaining material and system factors  $\mu_{crit}$  and  $k_{crit}$  for definition of the  $\mu$ : friction and  $k$ : wear coefficients. An attempt to visualize the described interaction was made in the graphical abstract.

### 3. Materials and Methods

#### 3.1. Materials

A polyoxymethylene homopolymer (POM) from DuPont (Delrin 100 NC010) and unfilled polyamide (PA46) from DSM (Stanyl TW300) were chosen as polymer materials. The tribological experiments were performed with POM and PA46 in ball-on-plate and pin-on-disc tests geometry. The polymer specimens were in contact with a steel tribosystem with a 100Cr6 steel ball (diameter  $\frac{1}{2}$ ”,  $R_a = 0.15 \mu\text{m}$ ;  $R_z = 1.4 \mu\text{m}$ ,  $R_{ku} = 3.85$ ,  $R_{Pc} = 37/\text{cm}$ ), which was integrated in the tribometer and used as a tribological partner. Axial bearing rings INA AS6590 with technical roughness (diameter of track 82 mm,  $R_a = 0.27 \mu\text{m}$ ,  $R_z = 2.4 \mu\text{m}$ ,  $R_{ku} = 4.0$ ,  $R_{Pc} = 193/\text{cm}$ ) were used as a tribological partner for pin-on-disc tests.

Polar polyalkylenglycole (pPG, viscosity  $\eta = 30 \text{ mm}^2/\text{s}$  at  $40 \text{ }^\circ\text{C}$ ), non-polar (nPG, viscosity  $\eta = 30 \text{ mm}^2/\text{s}$  at  $40 \text{ }^\circ\text{C}$ ), ester oil  $\eta = 30 \text{ mm}^2/\text{s}$  at  $40 \text{ }^\circ\text{C}$  (Ester, viscosity  $\eta = 23.5 \text{ mm}^2/\text{s}$  at  $40 \text{ }^\circ\text{C}$ ), and polyalphaolefin (PAO, viscosity  $\eta = 30 \text{ mm}^2/\text{s}$  at  $40 \text{ }^\circ\text{C}$ ) were obtained from Klüber Lubrication München SE and Co. KG, München, Germany.

The POM and PA46 specimens were prepared in the shape of rectangular plates ( $6 \times 4 \times 15 \text{ mm}^3$ ) for the ball-on-plate contact or cylindric pins for the pin-on-disc test (height 4 mm, diameter 5 mm), which were cut from molded plates (Konzelmann GmbH, Löchgau, Germany) by micro-abrasive-water cutting (Figure 1).

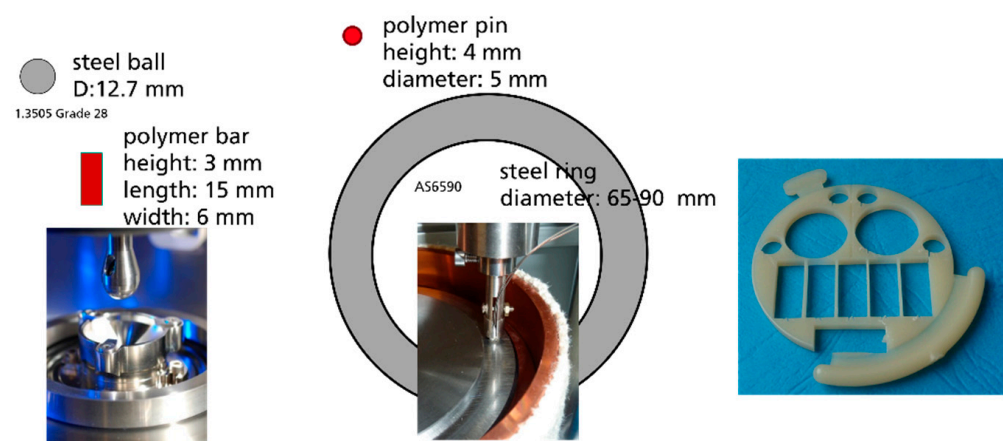


**Figure 1.** Tribological testing set-up: ball-on-plate and pin-on-disc experiments and polymer discs after cutting out of specimen (pins and bars, and not used rings).

All polymer specimens were dried at 70 °C in a chamber with less than 3 mbar gas pressure for 4 days. The specimens used for tribological and hardness experiments were conditioned in the lubricants and under N<sub>2</sub> atmosphere for 1000 h at 100 °C. The storage or conditioning for 1000 h at 100 °C or 96 h at 130 °C is named “stored” for all lubricants or “N2” for nitrogen gas atmosphere and will be used in combination with the thermoplastic. It should be noted here that the “stored” in the lubricant causes aging and sorption of the “soluble” polymers.

### 3.2. Tribological Experiments

Ball-on-plate experiments (Figure 1) were used to carry out oscillatory tribological experiments. A rotational rheometer developed by Anton Paar GmbH, Ostfildern, Germany, was used, which was equipped with a tribological measuring unit. In this way, very low but also high velocities and deflections (0.1 μm/s to 1.4 m/s) can be obtained by a rotation of a polished steel ball. To achieve stable and reproducible system conditions, a testing sequence was applied to form a run-in situation [5]. Conducting the oscillatory experiments in this range of sliding speeds (oscillatory mode) makes it possible to record friction data in the static friction and boundary-lubrication regimes. Using a data acquisition rate of 10 data points per decade, the loading torque was increased on a logarithmic scale at an oscillation frequency of 1 Hz. The repeatability was tested for each system by a series of 5 transitions from sticking to gliding (resulting, e.g., in a standard deviation of 10% for POM and nPG).

Pin-on-disc tests (Figure 1) were used to characterize the lubricated polymer contact. The tribometer is a custom-made device that can be used for high temperatures up to 250 °C, requiring only small amounts of lubricant and different sizes of axial bearings as the counterpart. Carrying out a continuous measurement of the pin height with an inductive displacement transducer, wear depths >0.1 μm can be recorded, however, requiring a long measuring time. A wear and friction map by variation of  $v$  and  $p$  was recorded prior to the wear test to check the applicability of the 3-factor model and choose the testing conditions for run-in measurements.

Friction and wear maps were recorded to be able to choose a mild loading scenario for the run-in condition. Mild loading should show a high transfer-film forming ability, a low but measurable wear rate and prevent frictional heating. The maps (Figure 2) were obtained from a 5-day test procedure for each system. Increasing load levels (1, 3, 10 MPa) and decreasing velocities were chosen. In this way, a continuously increasing frictional power density was applied to the frictional surface and an increasing roughness interference was achieved. The mild loading conditions at  $p = 3$  MPa and velocity  $v = 0.25$  m/s result in low friction values that induce a frictional heating of less than 10 K. The resulting dependence of the friction and wear coefficients could be parameterized by the chosen 3-factor model (7) and (8). Both factors had to be used to describe the transition behavior in mixed lubrication with respect to viscosity  $\eta$  and the mechanical interaction intensity with respect to surface hardness  $H$  for all combinations of  $p$  and  $v$ . In this context, the chosen wording “minimal” 3-factor model was validated.

The running-in pin-on-disc tests were performed for 4 h at room temperature with a pressure  $p = 3$  MPa at  $v = 0.27$  m/s. If the coefficient of friction stays below  $\mu = 0.1$ , frictional temperature calculations according to [3] result in an increase in polymer surface temperature less than 15 K. The selected mild loading condition will result in run-in states for at least the second half of the duration of the experiment and estimated wear rates of about 1 μm/h.

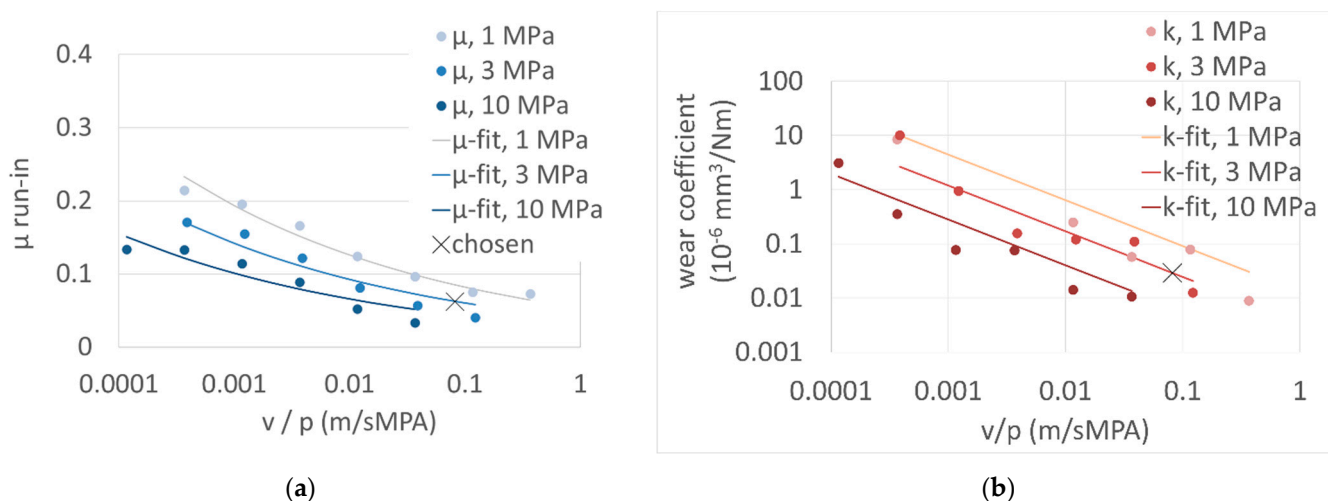


**Figure 2.** Single-specimen maps of run-in friction (a) and wear coefficient  $k$  (b) of PA46 lubricated with PAO.

### 3.3. Indenter Measurements

Indentations were performed with a Fischerscope H100C Xyp. The test was performed with a Vickers indenter, which generates indentations of a few  $\mu\text{m}$  into thermoplastics for a load of 75 mN. Indentations were carried out on a matrix grid, to generate statistically comparable results for the surface and the underlying morphology and composition. Marten's hardness can directly be derived from the applied force  $F$  and indentation depth  $h$  by  $HM = F/26.4 h^2$ . Reduced elastic modulus  $EIT$  and Vickers hardness  $HV$  of plastic behavior can be derived in a standardized way from the indentation curve [22]. A matrix of 20 indentation points was applied on injection-molded surfaces and cut surfaces. The resulting hardness measurements show a standard deviation of 22% for POM. A standard deviation of 6% for POM was found after flattening the tested area by a run-in wear experiment.

### 3.4. Contact Angle Measurements

The sessile drop method placing 2  $\mu\text{L}$  droplets on the samples was used on a contact angle measurement device produced by Data Physics GmbH, Filderstadt, Germany. Three standard liquids (water [23], ethylene glycol [23] and diiodomethane [24]) were used to characterize the unknown surface and interfacial energies. The droplet profile is recognized and recorded by the software of the instrument, and the contact angle is calculated automatically. All the calculations and interpolations were carried out according to Equations (3)–(8). A detailed description of the procedure was given in the previous study [5]. The robustness of the standard regression method of surface and cohesive energies was increased by including measurements on float glass, PTFE-foils and Mg-PSZ ceramic surfaces and fitting all parameters in all equations simultaneously with shared parameters.

### 3.5. Mass Uptake

To measure the uptake of the lubricants by the thermoplastics and to calculate Fick's diffusion coefficient, specimens of POM and PA46 with a thickness  $l$  of 600  $\mu\text{m}$  were first pre-dried at a temperature of 70  $^{\circ}\text{C}$  and a gas pressure less than 3 mbar until a weight equilibrium was reached. The specimens were then weighted, immersed in the lubricants and stored in ovens at the temperature of interest (here: 100  $^{\circ}\text{C}$ ) for up to 105 days. During storage, a constant flow of nitrogen gas passed through the lubricants along the specimens to suppress thermo-oxidative aging. Specimens were removed from the ovens at increasing time intervals, cleaned in the same manner, and weighed. The mass fraction of lubricant in the specimen can be recalculated from the mass data and fitted [25] by (8) to fit Fick's diffusion coefficients.

### 3.6. Dynamic Mechanical Analysis

The temperature dependence of the real ( $G'$ ) and imaginary part ( $G''$ ) of the complex dynamic shear modulus ( $G^* = G' + iG''$ ) of POM and PA46 was measured by a dynamic mechanical analyzer of type ARES (TA Instruments, Newcastle, United States) at a frequency of 1 Hz. Specimens of POM and PA46 were pre-dried as described above and analyzed in a temperature range from  $-140$  to  $100$  °C and  $0$  to  $220$  °C, respectively. The heating rate was  $1$  K/min. Measurements were performed under a nitrogen gas atmosphere. In this work, only the values at  $20$  °C are used for interpretation.

### 3.7. Applied Correlation Method

If not stated otherwise, all data refer to properties at  $25$  °C and all experiments were performed at  $25$  °C. The values of  $R^2$  in the diagrams are the coefficient of determination defined by regression theory for linear or exponential fits to allow a linearity test of the chosen diagram. The use of  $R^2$  is helpful, but it should be interpreted with caution since it will be used for 3 to 4 different lubrication systems and systematic deviations and non-statistic errors should be expected.

## 4. Results and Discussion

### 4.1. Contact Angle Measurements and Interaction Energies

As stated above, the work of spreading  $W_{spreading}$  (2) and the work of solving  $W_{solving}$  (3) can be determined from surface- and interfacial energies, which in turn are determined by contact angle measurements. All calculations and interpolations for the interaction energies were carried out according to the procedure described by Wahed et al. [5], and the resulting energies are summarized in Table 2.

**Table 2.** Table of lubricant characteristics.

| lubricant or Body | Viscosity<br>at $40$ °C<br>( $\text{mm}^2/\text{s}$ ) | Cohesive or Surface Energy          |  | PA46                               |                                      | POM                                |                                      |
|-------------------|---|-------------------------------------|--|------------------------------------|--------------------------------------|------------------------------------|--------------------------------------|
|                   |   | $\gamma$ Polar<br>( $\text{mN/m}$ ) | $\gamma$ Dispersive<br>( $\text{mN/m}$ ) | $W_{solving}$<br>( $\text{mN/m}$ ) | $W_{spreading}$<br>( $\text{mN/m}$ ) | $W_{solving}$<br>( $\text{mN/m}$ ) | $W_{spreading}$<br>( $\text{mN/m}$ ) |
| PAO               | 30  | 0.6                                 | 31.5                                     | 11.3                               | 13.0                                 | 1.7                                | 5.1                                  |
| Ester             | 23.5  | 0.7                                 | 31.6                                     | 10.7                               | 12.1                                 | 1.5                                | 4.5                                  |
| nPG               | 30  | 0.27                                | 30.1                                     | 12.7                               | 15.3                                 | 2.3                                | 6.5                                  |
| pPG               | 30  | 1.4                                 | 34.7                                     | 9.1                                | 9.9                                  | 1.0                                | 3.4                                  |
| PA46              | -   | 16.4                                | 24.8                                     | -                                  | -                                    | -                                  | -                                    |
| POM               | -   | 4.2                                 | 29.3                                     | -                                  | -                                    | -                                  | -                                    |
| Steel             | -   | 6.8                                 | 25.2                                     | -                                  | -                                    | -                                  | -                                    |

The closer the solubility parameters of the polymer and lubricant, the more likely the polymer can be solved in the lubricant. The interaction radius  $R$  depends on the type of polymer. The surface and the cohesion energy  $\gamma$  of the polymer or liquid and its dispersive, polar contributions and hydrogen bonding contribution are correlated to the Hansen solubility parameter (5) [19]. The sorption of lubricant in the polymer is also related to the dispersive, polar interactions and hydrogen bonding (which is usually neglected) between the molecules since solution and sorption have similar molecular origins. The corresponding interactions are expressed in the work of solving  $W_{solving}$ , which can also be used as a measure of the sorption ability of the lubricant within the actual polymer matrix.

With increasing values of the work for spreading (spreading energy:  $W_{spreading}$ ), the tendency for spreading decreases, which leads to an increase in adhesive contacts in the frictional contact.

For the lubricants studied, the following trends regarding spreading and solving (sorption) can be seen for POM and PA46: POM has a mild solving/sorption and a mild spreading tendency, whereas PA46 has no solving/sorption and no spreading tendency.

The consequences of these trends on the tribological behavior will be considered below, regarding the hypotheses formulated above.

#### 4.2. Mass Uptake

In Figure 3, the relative mass uptake  $\phi$  versus time is shown for POM (a) and PA46 (b) during isothermal storage in the lubricant indicated or in nitrogen atmosphere (PA46) for up to 105 days at 100 °C. The time-dependence of the mass uptake is a measure of the diffusive transport (diffusion coefficient) and the equilibrium sorption for a given lubricant within the semicrystalline polymer. Both are coupled to the free volume of the amorphous phase. By fitting the data using Equation (8) (dotted lines in Figure 3a), the equilibrium values of the relative mass uptake  $\phi_\infty = \phi(t \rightarrow \infty)$  and the diffusion coefficients are estimated for the systems that show a mass uptake (Table 3). Since the sorption–time curve of ester oil in POM cannot be fitted properly by the diffusion equation, the values for the mass uptake after 105 days of storage time  $\phi_{105d} = \phi(t = 105d)$  are used for further interpretation and given in Table 3.  $\phi_{105d}$  is within a range of 6% to  $\phi_\infty$ . As shown in Figure 3b for PA46, no mass uptake but a slight mass loss is detected for the organic lubricants studied as well as for storage (thermal aging) under nitrogen atmosphere. Therefore, no measurable solution of significant amounts of the PA46 or additives in the lubricants (acting as solvents) was found. The results of the sorption experiment for POM can be summarized as follows: The diffusion coefficients of the lubricants in POM increase with increasing polarity (see Table 2), and the tendency for sorption is coupled to the solvating energy. As expected from the parameters in Table 2, PA46 does not show a sorption tendency in the experiments. The slight mass decrease can be explained by diffusion (extraction) of additives or degradation products (including residual water) into the lubricants.

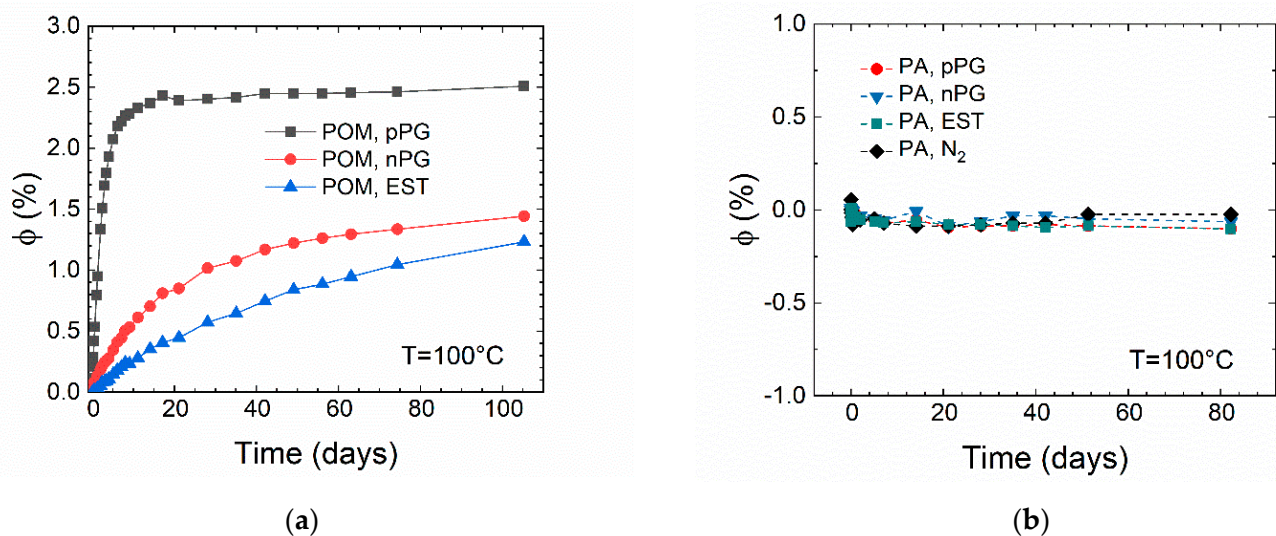


**Figure 3.** Relative mass uptake  $\phi$  versus time for POM (a) and PA46 (b) during storage in the lubricant indicated or in nitrogen atmosphere (PA46).

**Table 3.** Diffusion and sorption of lubricant in POM at 100 °C.

| Lubricant | Diffusion Coefficient D<br>( $10^{-13} \text{ m}^2/\text{s}$ ) | Equilibrium Sorption $\phi_\infty$<br>(%) | Sorption $\phi_{105d}$<br>(%) |
|-----------|--|---|-------------------------------|
| Ester     | –  | –   | 1.23                          |
| PAO       | 0.61   | 0.1                                       | 0.105                         |
| nPG       | 0.11   | 1.53                                      | 1.45                          |
| pPG       | 1.22   | 2.45                                      | 2.51                          |

As a pragmatic solution, the value of relative mass uptake for sufficiently long times  $\phi_{105d} = \phi(t = 105d)$  is plotted versus the solving energy  $W_{solving}$  for different polymer–lubricant pairings (Figure 4). POM (with  $W_{solving} < 5$  mN/m for all lubricants) shows a significant mass uptake for pPG, nPG and Ester, which is decreasing with increasing values of  $W_{solving}$ . Surprisingly, a low mass uptake was measured for PAO. Therefore, the applicability on more systems was tested and confirmed with a different supplementary system PK/pPG (polyketone). However, for PA46 systems, no significant uptake of oil was measured after storing in nitrogen. This finding confirms the hypothesis for the sorptive POM-systems that the tendency for sorption of lubricants can be expressed by  $W_{solving}$ . The solving tendency seems to be well correlated in a logarithmic or at least power dependence to the mass uptake:  $\phi_{105d} \sim \exp(-W_{solving})$ .

On the other hand, there is no swelling observed for PA46 by all organic lubricants. In this case,  $W_{solving}$  should be related to local interfacial interactions.

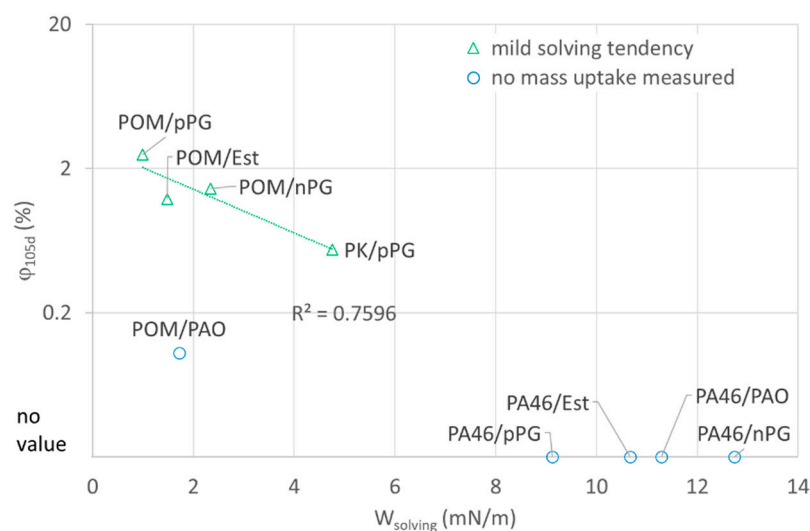


**Figure 4.** Relative mass uptake  $\phi_{105d}$  versus solving energy ( $W_{solving}$ ) for different polymer–lubricant pairings after an estimated long-time storage in the lubricant indicated by the labels. The systems that showed no mass uptakes were included to visualize the range of theoretical extrapolation of possible uptake for PA46 systems.

#### 4.3. Hardness Measurements

To study solving, sorption, the related plasticization and thermal aging effects, the hardness was measured following the results of Bormuth et al. [6]. In order to distinguish near-surface effects from bulk effects, specimens were cut, and the indentations were carried out on the cut surface 300  $\mu\text{m}$  below the sample surface. For sorptive polymer–lubricant pairings, plasticization is expected to be observable within the bulk (here 300  $\mu\text{m}$  below the surface), whereas for samples without sorption, changes in hardness at 300  $\mu\text{m}$  below the surface are expected to represent effects due to thermal aging (i.e., chemical reactions and/or post-crystallization). Shear flow and/or thermal conditions during injection molding are known to lead to morphology gradients within the sample, such as oriented structures and differences in crystallinity. In a separate study, the depth dependence of the hardness for swollen and unswollen POM was investigated. The depth-depending changes in the hardness due to sorption and plasticization are found to considerably exceed those due to spatial changes in the crystallinity. If the crystallinity differences are small, the processing-induced hardness gradients are of second order for sorption-induced mechanisms since lubricant transport and sorption take place in the amorphous phase of the semicrystalline polymer.

The Martens' hardness ( $HM$ ) is expected to reflect both elastic deformation and—to a smaller extent—plastic deformation, whereas the Vickers hardness ( $HV$ ) is rather related to

plastic deformations. This allows a certain separation between (possible) elastic ( $HM$ ) and plastic ( $HV$ ) contributions.

Figure 5 shows the Martens' ( $HM$ ) and Vickers ( $HV$ ) hardness at a depth of 300  $\mu\text{m}$  below the sample surface after storage in the lubricants or under a nitrogen atmosphere. Since for PA46 no sorption could be measured, the hardness data are not plotted versus lubricant uptake.

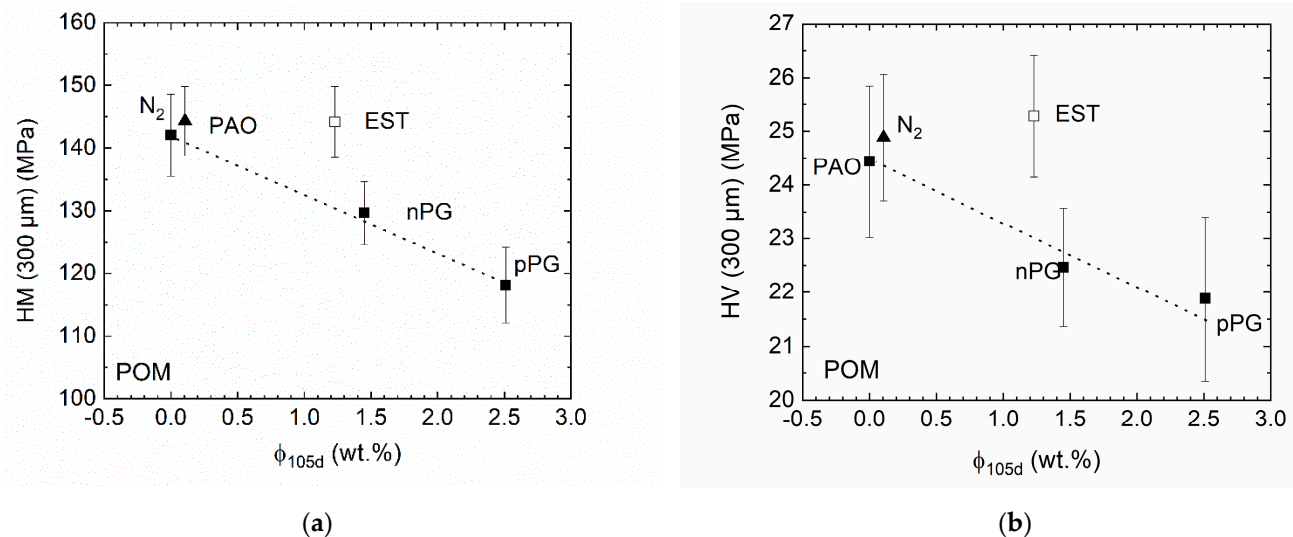


**Figure 5.** (a) Martens' ( $HM$ ), and (b) Vickers hardness ( $HV$ ) at a depth of 300  $\mu\text{m}$  below the surface versus the relative mass uptake  $\phi_{105d}$  after storage in the lubricant or nitrogen atmosphere.

As expected,  $HM$  and  $HV$  are both decreasing due to the plasticization of the POM with the lubricant absorbed in the polymer matrix. It is surprising that with the exception of ester (open symbols), this seems to be independent of the detailed chemical structure of the lubricant (specific volume, polarity, etc.). The deviation of the POM-ester pair could be explained by a lower tendency for plasticization for the same amount of the sorbate or a simultaneous counteracting hardening due to chemical aging (e.g., crosslinking) accelerated by the ester oil. In comparison, for the thermal aging in PAO (which is almost not swelling POM) and under nitrogen, only a slight increase in the hardness due to thermal aging can be found. The difference can possibly be explained by the differences in heat transfer or different transport and solubility properties of reaction products in PAO.

Based on these data, the ratio of Martens' hardness of samples stored in lubricants ( $HM_{stored}$ ) and the pristine ones ( $HM$ ) are plotted in Figure 6 versus the solving energy  $W_{solving}$  to differentiate between aging effects. The samples stored in oil are assumed to have reached equilibrium sorption.

The significant decrease in  $HM_{stored}/HM$  for the POM-lubricant pairings ( $W_{solving} < 5 \text{ mN/m}$ ) with decreasing  $W_{solving}$  reflects the swelling tendency of those systems (see Figure 3). Thus,  $W_{solving}$  is for the POM-pairings an (inverse) measure of the sorption tendency of organic lubricants.

In contrast to the sorptive POM-lubricant pairings, the ratio of  $HM_{stored}/HM$  for the non-sorptive PA46-pairings (see also Figure 6) tends to increase with  $W_{solving}$ . It should be emphasized that the hardness at 300  $\mu\text{m}$  depth is a bulk rather than a surface property, and no significant bulk changes were observed during thermal storage. The oil dependence of  $HM_{stored}/HM$  from  $W_{solving}$  could be related to a migration from the polymer into the lubricants related to the solubility of reaction products (or reactants) or to sorption in the polymer. However, since the amorphous phase of POM is at room temperature in a rubber-like state, and the amorphous phase of dry PA46 is in the glassy state, the higher plastic hardness  $HV$  of PA46 systems and significant differences in transport behavior between POM and PA46 is not surprising.

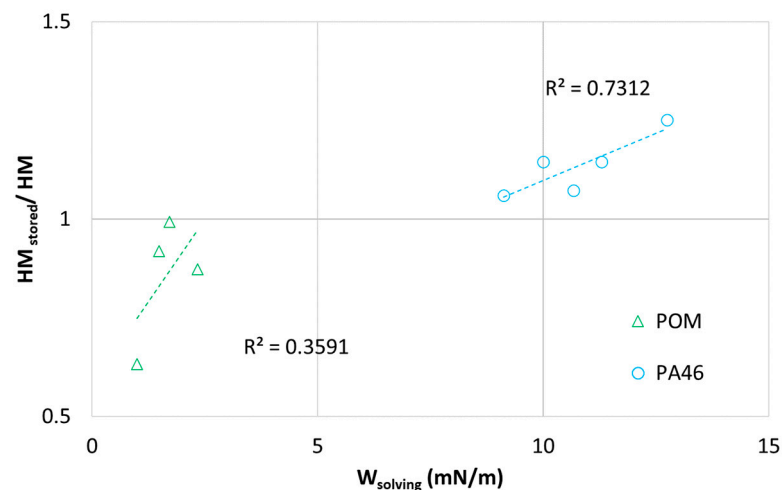


**Figure 6.** Dependence of the relative Martens' hardness ( $HM_{stored}/HM$ ) for POM (open triangles) and PA46 (open circles) versus  $W_{solving}$  after storage in oil.

As stated above, the measurement of Martens' hardness ( $HM$ ) and Vickers hardness ( $HV$ ) at the same position allows a certain separation between possible elastic ( $HM$ ) and plastic ( $HV$ ) contributions. Therefore, in Figure 7,  $HM$  is plotted versus  $HV$  measured at a depth of  $300\ \mu\text{m}$ . It can be concluded that the swelling and the related plasticization of the POM-pairings (open triangles in Figure 7) are accompanied by a reduction in both elastic and plastic contributions (related to  $HM$ ). The corresponding comparison between unaged POM and POM stored in a nitrogen atmosphere (filled triangles) shows a strong reduction in the plastic fraction, represented by the Vickers hardness ( $HV$ ), while the Martens' hardness  $HM$  is almost unchanged by the thermal treatment. One possible explanation is an increase in chain mobility responsible for shear or creep, which is due to the degradation of chains in the rubbery amorphous phase of POM without any significant change in rubber-elasticity. In pristine PA46, the amorphous phase is in the glassy state, and the degradation during aging may increase both elastic ( $HM$ ) and plastic contribution ( $HV$ ).

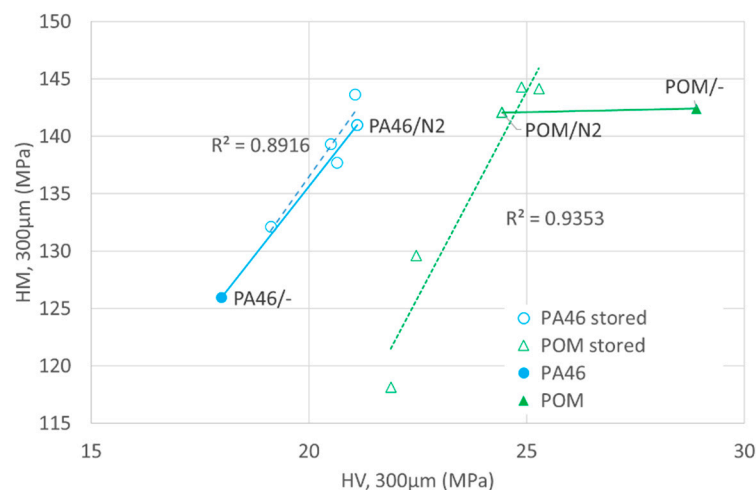


**Figure 7.** Martens' hardness ( $HM$ ) versus Vickers hardness  $HV$  (both measured  $300\ \mu\text{m}$  below the surface) for PA46 (triangles) and POM samples (circles). The open symbols label samples that are stored in the oil or nitrogen. The closed symbols indicate pristine samples (-).

However, there is a similar reduction in the Martens hardness for PA46 without any swelling for the polar lubricant pPG (open symbols). The reason for this reduction in hardness for PA46 is not yet understood and is possibly related to the above-mentioned

differences in different interface transfer and/or solubility of reaction products (or reactants) for lubricants with different  $W_{solving}$ . One may speculate on chemical degradation by the interplay of chain scission and post-condensation, which are well-known for polyamides, and/or changes in crystallinity by thermal aging and/or degradation-driven so-called “chemo-crystallization”. The assumption of diffusion-controlled chemical aging or structural changes by thermal treatment in non-swollen PA-pairings is supported by the significant difference between the unaged PA46 sample and a sample stored under nitrogen without oil (filled symbols).

#### 4.4. Dynamic Shear Modulus

In Figure 8, the real part of the dynamic shear modulus  $G'$  of POM, measured at 1 Hz at 20 °C, is plotted versus the relative mass uptake  $\phi_{105d}$ . The samples were stored in oil at 100 °C. The reduction in the real part  $G'$  of the shear modulus for POM with  $\phi_{105d}$  in the different lubricants correlates with the reduction in Marten’s hardness in Figure 5. The significant increase in  $G'$  due to aging under nitrogen (without oil) is surprising since the Marten’s hardness  $HM$  that covers elastic and partially plastic behavior did not show such a strong increase. However, there is a significant reduction in plastic behavior represented by  $HV$ .  $G'$  is a bulk property representing the response of an amorphous and crystalline phase to a shear deformation, and an increase in  $G'$  can, therefore, be related to chemical or physical crosslinking in the rubber-like amorphous phase and/or an increase in crystallinity.

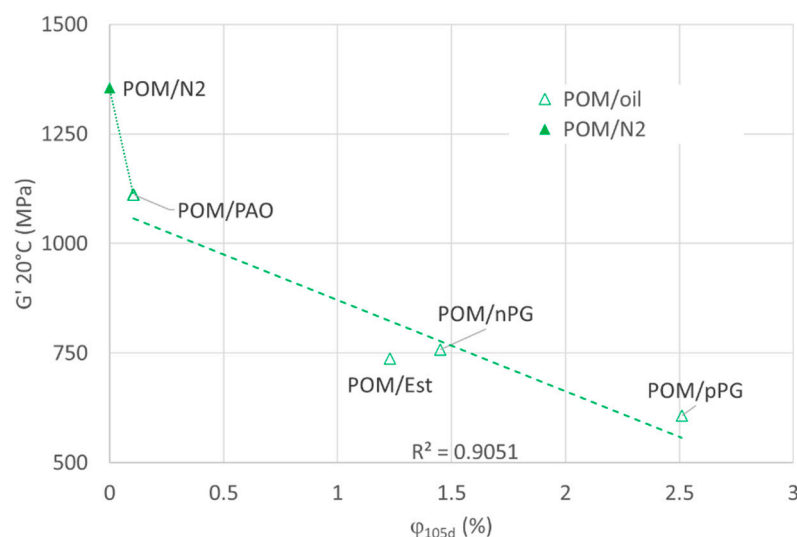


**Figure 8.** Shear modulus  $G'$  versus relative mass change  $\phi_{105d}$  (lubricant uptake to saturation). In addition to stored polymer–lubricant pairs, samples stored under nitrogen atmosphere (filled symbols) are included in the graph.

Figure 9 plots the shear modulus  $G'$  against the Vickers hardness ( $HV$ ) at 300  $\mu\text{m}$  depth for samples stored in oil and in nitrogen. The shear modulus values are for a temperature of 20 °C, which is above the glass transition temperature for POM in the plateau region, where the amorphous phase is in a rubbery state.

A comparison of the different pairings and conditioning procedures reveals the following: For POM (green symbols) stored in sorptive oils (nPG and pPG) a reduction in  $G'$  roughly correlating with  $HV$  is observed due to plasticization. For PA46 (blue symbols) stored or in the different lubricants, hardness and modulus change only for pPG to a relevant extent and in a similar way as for POM. In contrast, thermal aging in a nitrogen atmosphere without oil results for POM and PA46 (filled symbols) in an opposing trend:  $G'$  decreases with reduction in plastic  $HV$  hardness at a depth of 300  $\mu\text{m}$ . The simultaneous reduction in  $G'$  and  $HV$  for sorptive lubricants such as pPG can be related to plasticization, whereas the increase in  $G'$  and the decrease in  $HV$  can be attributed to thermal aging

(changes in chain or superstructure) in the bulk without significant swelling. For the latter, the changes in the shear modulus and  $HV$  are not coupled in a simple manner.

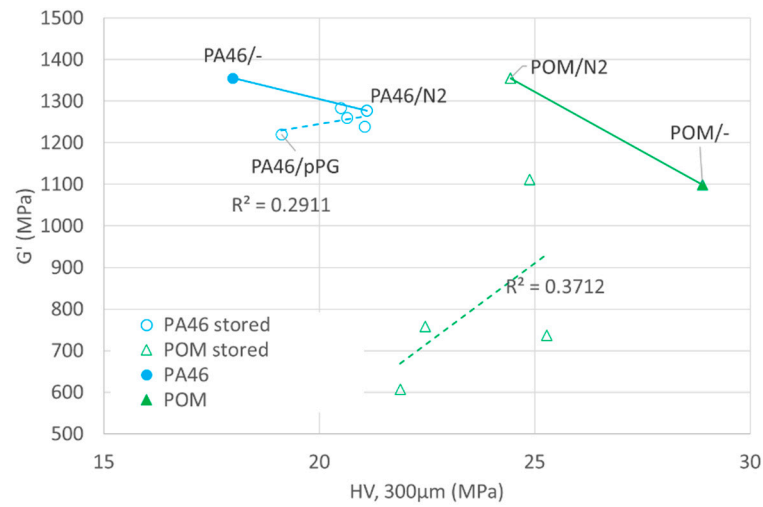


**Figure 9.** Dependence of shear modulus  $G'$  on Vickers hardness at a depth of  $300\ \mu\text{m}$  for POM (blue circles) and PA46 (green triangles). A comparison of unaged samples and samples after thermal aging without oil (filled symbols and (-)) and those stored in oil (open symbols).

#### 4.5. Static Friction and the Onset of Gliding

An essential question for the investigation of the transition from static to dynamic friction is the detection of the onset of gliding. By using an oscillatory deflection method, the transition from sticking to gliding can be investigated by repeating the transition events several times. That way, one can distinguish between the elastic sticking and viscous gliding response of the system. The beginning of the gliding motion was defined at  $\tan(\delta) \sim 1$  in the oscillatory experiment, which is the tangent of the phase angle between oscillatory excitation and the sample response.

PA46 (blue circles), which does not show mass uptake in the organic lubricants, shows an increase in  $\mu_{stiction}$  in Figure 10 with the spreading energy for both the samples stored in the lubricants as well as the pristine samples (open circles). Since the tendency for spreading decreases with increasing values of  $W_{spreading}$ , the positive slope can be explained by an increase in the adhesive contact with decreasing spreading.

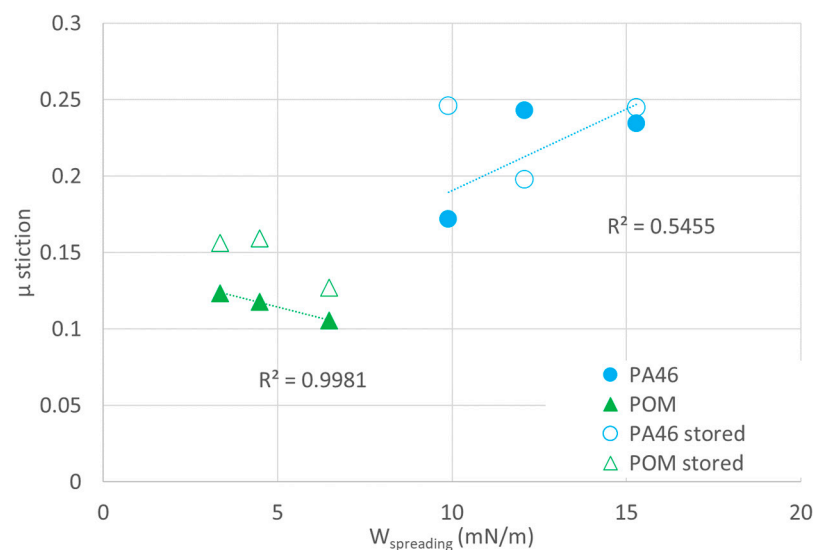


**Figure 10.** The  $\mu_{stiction}$  as a function of the spreading energy for POM (triangles) and PA46 (circles) before (filled symbols) and after storing in oil (open symbols) measured at room temperature.

The POM-lubricant pairings, which show significant sorption for most of the studied lubricants, do not show the expected dependence on the spreading energy for both samples swollen in the lubricants (open triangles) and pristine samples (filled triangles). The values of  $\mu_{stiction}$  for the swollen samples are somewhat higher than those for the unswollen ones because of swelling of the polymer chains at the surface of a sorptive polymer) (here, for POM, sorption is expected to occur immediately. The sorption of the lubricants is expected to occur preferentially in the rubber-like state of the amorphous phase of POM and is related to  $W_{solving}$ , and in such a case,  $W_{spreading}$  is not relevant.

In Figure 11,  $\mu_{stiction}$  is shown as a function of the spreading energy for PA46 measured at room temperature (blue circles) and at 100 °C (red circles). At room temperature, dry PA46 is tested below its glass transition temperature ( $T_g$ ), whereas at 100 °C, it is tested above  $T_g$ . The chain mobility is almost frozen in the glassy state, and therefore, the increase in the adhesive contact with decreasing spreading is a dominant mechanism (see Figure 11). Above the glass transition temperature (red symbols), the chain mobility is expected to become more important. The temperature dependence of a rate and state conditions is the reason for lower values of  $\mu_{stiction}$  at 100 °C [5]. Such an increase in chain mobility is similar to plasticization by sorption of an organic liquid, with similar effects on stiction as plasticization by a “solvent”. Unfortunately, the surface energy of PA46 at 100 °C could not be measured by contact angles to test the concept of interaction energies below to above the glass temperature. An equivalent test for POM was not possible since the glass temperature was as low as  $-70$  °C. It should be mentioned that above the glass transition temperature, solvent transport becomes easier, and an additional plasticization effect cannot be excluded.

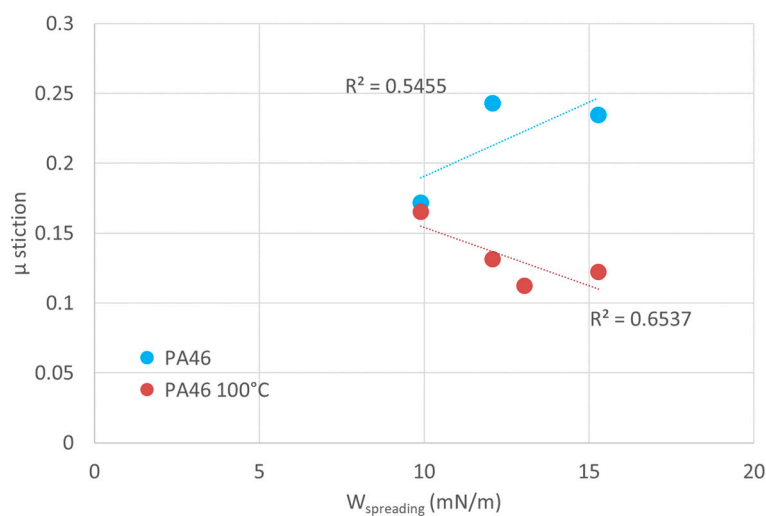


**Figure 11.** Comparison of  $\mu_{stiction}$  measurements for PA46 at room temperature (blue circles) and at 100 °C (red circles), which is, for PA46, above the glass transition temperature.

#### 4.6. Wear Experiments

In the following graphs, the results of the tribological run-in experiments are summarized with respect to the solving tendency, stiction, hardness and sorption, as well as to the imaginary part of the complex dynamic shear modulus  $G'$  and  $G''$ . Four wear experiments were performed for each system.

To systematize the tribological results,  $W_{solving}$  is used in Figures 12 and 13 as an indicator for sorption, solubility and plasticization but also for degradational mechanisms. The run-in wear rate shows a tendency to decrease with increasing solving energy  $W_{solving}$ . The wear rate is somewhat lower for the pristine samples. For the POM-pairings, the decrease in wear rate with  $W_{solving}$  can be related to the plasticization by the lubricants, which is also expected for the upper layers of the pristine sample due to the lubricant applied during the experiment. The swelling and plasticization are expected to increase the contact and/or to lower the chain interactions responsible for cohesive failure. The

reason for the decrease in the wear rate with increasing  $W_{solving}$  for the PA46-pairings is not clear yet. However, one may speculate that near-surface interactions such as hardening by chemical and/or morphological changes in crystallinity as well as brush-like dangling or solvated chains, etc., which are represented as well in  $W_{solving}$ , influence the wear rate.

In Figure 13, no systematic correlation between the friction coefficient ( $\mu_{run-in}$ ) and solving energy for the stored POM samples was found. For PA46, which is not swollen by the lubricants,  $\mu_{run-in}$  appears to have a slight tendency to increase with the solving energy solely because of the spreading behavior. For the others, an increase in  $\mu_{run-in}$  with the solving energy should indicate polymer–lubricant interface interactions localized close to the surface and, in the case of POM, related to property changes due to sorption and plasticization in the bulk.

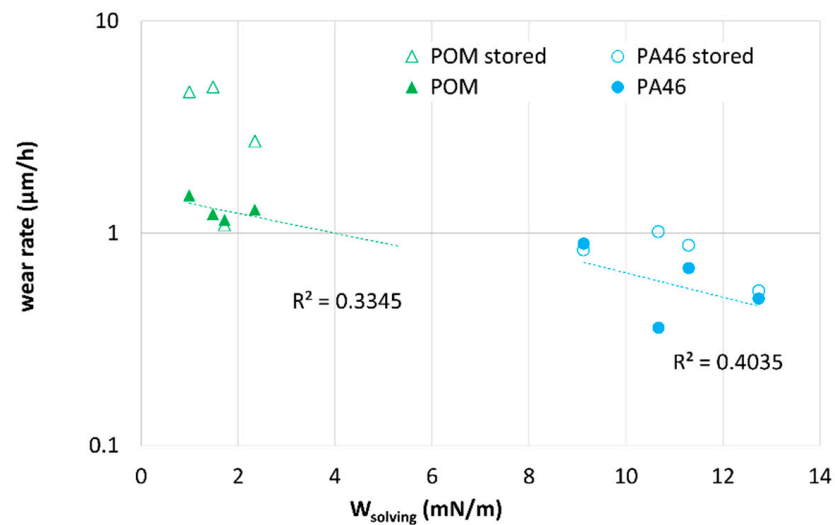


**Figure 12.** Run-in wear rate versus  $W_{solving}$  for different POM-lubricant (triangles) and PA46-lubricant pairings (circles) measured at room temperature versus solving energy (experimental parameters: 3 MPa, 0.25 m/s, 4 h) for samples stored in the lubricants (open symbols) and pristine samples (filled symbols).

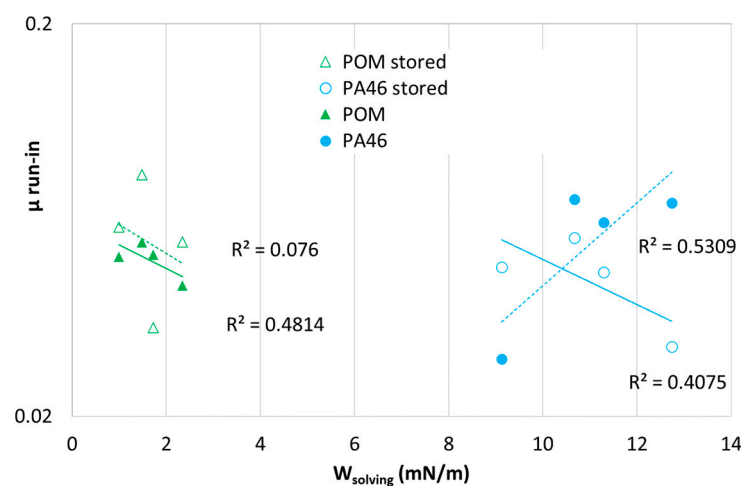


**Figure 13.** Friction versus  $W_{solving}$  for different POM-lubricant (triangles) and PA46-lubricant pairings (circles) measured at room temperature versus solving energy (experimental parameters: 3 MPa, 0.25 m/s, 4 h) for samples stored in the lubricants (open symbols) and pristine samples (filled symbols).

In Figure 14, the run-in wear rate is plotted versus  $\mu_{stiction}$  for POM (triangles) and PA46 (circles) of pristine samples (filled symbols) and samples after storage in the lubricants

measured at room temperature. For adhesive wear, a positive slope of the run-in wear rate versus  $\mu$  stiction is expected. For the POM-lubricant pairings (triangles), the run-in wear rate increases with  $\mu$  stiction for pristine samples (filled symbols) and samples stored in the lubricants (open symbols). The trend is heavily pronounced for the plasticized POM samples and should be related to an increased contact area or a lower cohesion energy due to plasticization. On the other hand, the wear rate is almost independent of the stiction for the non-plasticized PA46-pairings. Here, adhesive friction has a minor impact.

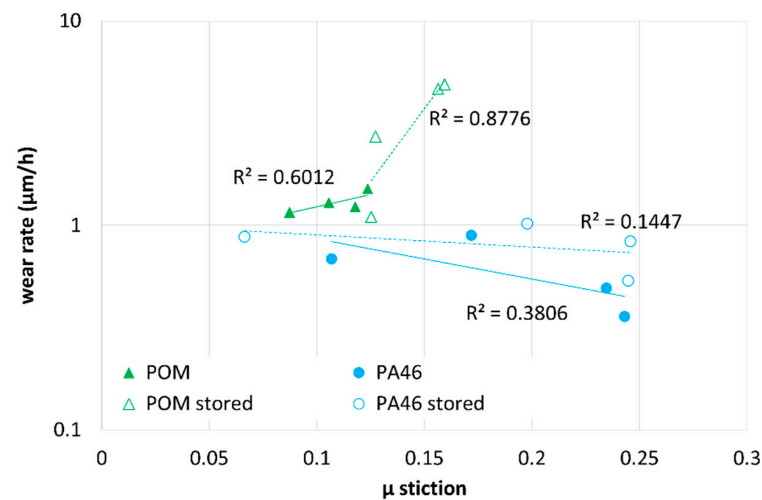


**Figure 14.** Run-in wear rate versus  $\mu$  stiction for POM (triangles) and PA46 (circles) prior to (filled symbols) and after storage in the lubricants (open symbols).

In Figure 15, the run-in wear rate is plotted versus the ratio  $HM_{\text{stored}}/HM$  for samples stored for POM (triangles) and PA46 (circles). With an increasing surface hardness ratio ( $HM_{\text{stored}}/HM$ ), the run-in wear rate does decrease. It is generally expected that an increase in the surface hardness leads to a decrease in real contact area and, consequently, to a reduction in the wear rate. In the case of POM-lubricant pairings, the softening due to mass uptake and plasticization leads to the expected increase in the wear rate (Figure 16).

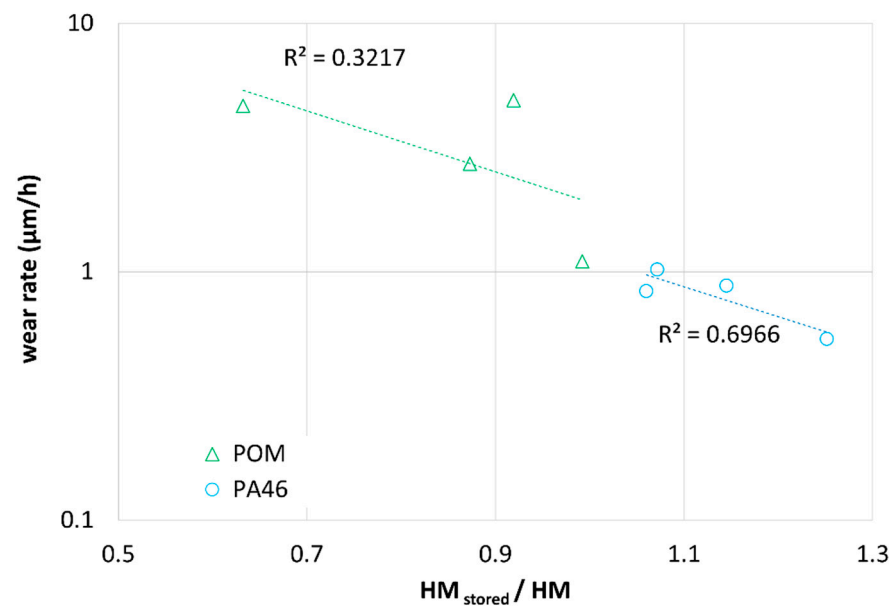


**Figure 15.** Run-in wear rate versus the ratio of Martens' hardness at the surface for samples stored in the lubricants and pristine ones ( $HM_{\text{stored}}/HM$ ) for POM (triangles) and PA46 samples (circles) measured at room temperature.

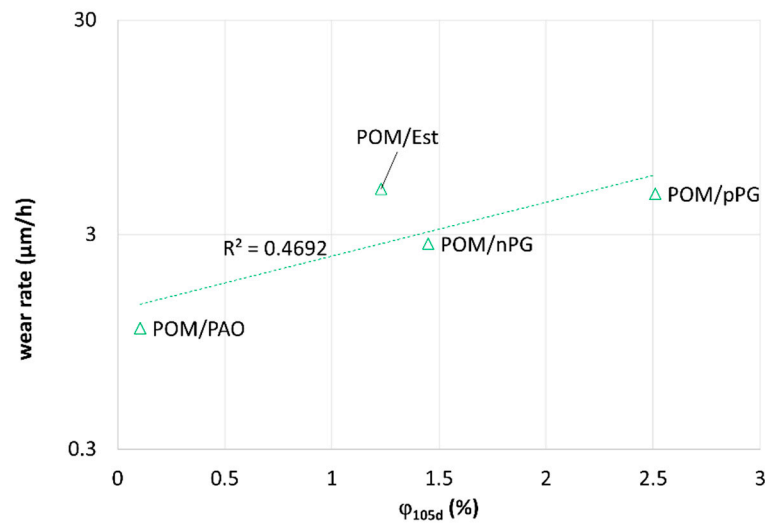


**Figure 16.** Run-in wear rate versus relative mass uptake  $\phi_{105d}$  for different POM-lubricant pairings stored in the lubricant.

For the non-swelling PA46-lubricant pairings, a lower wear rate is found for a higher surface hardness. The increase in  $HM_{stored}/HM$  for PA46 can be explained by structural changes close to the surface or in the bulk due to thermal treatment (e.g., by crosslinking or post-crystallization) and are represented by the surface hardness. For polyamides, the chemical and structural aging effects such as crosslinking by post-condensation and chain scission at higher temperatures are well-known.

To test the hypothesis that the friction coefficient is related to the viscoelastic loss within the polymer, the run-in friction was plotted versus the imaginary part of the shear modulus  $G''$  for POM-lubricant pairings (circles) stored in oil. For the POM-lubricant pairings, saturation by sorption is almost received. The  $G''$  data represent measurements of the stored samples at 20 °C and 1 Hz. However, the data scattered significantly and ( $R^2 < 0.1$ ) no dependence on the run-in friction on  $G''$  was found.

In Figure 17, the run-in friction is plotted versus  $\mu$  stiction for specimens stored in oil (open symbols). It was found that run-in friction increases only for plasticized systems (POM) with the adhesion friction  $\mu$ . No change was found for pristine POM as well as for pristine and aged PA46 (Not shown,  $R^2 < 0.14$ ).

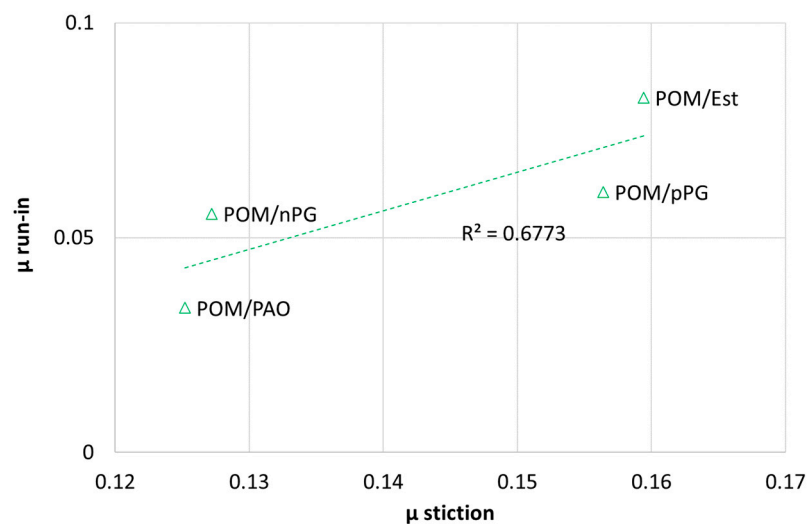


**Figure 17.** Dependence of run-in friction and on  $\mu$  stiction for pristine and stored in oil conditions of POM.

#### 4.7. Discussion for the Sorptive Polymer-Lubricant Pairings

The POM-lubricant pairings with Ester, nPG and pPG show significant sorption of the lubricants within the polymer matrix. The sorption tendency is related to the solving energy of these pairings. Values of  $0 \text{ mN/m} < W_{\text{solving}} < 5 \text{ mN/m}$  can be classified as sorptive POM-lubricant pairings. For these pairings, even small amounts of lubricants in the polymer matrix can change the tribological behavior significantly. Spreading by the lubricants, which is related to the spreading energy, is only a secondary effect of friction and wear for these pairings.

The sorptive polymer-pairings (POM with Ester, nPG and pPG) show an increasing wear rate and an increase in the run-in friction with increasing amount of lubricant absorbed by the polymer matrix (expressed by a decrease in  $W_{\text{solving}}$ ). The swelling of POM (high values of  $\phi_{\infty}$  and low values of  $W_{\text{solving}}$ ) results in a decrease in interchain forces, shear modulus and hardness. Thus, swelling leads to a higher real contact area and consequently to a higher wear rate and a larger value of run-in friction. In addition, the hardness can change due to thermal degradation, which can occur during thermal treatment in oil as well as in a nitrogen atmosphere.

#### 4.8. Discussion for the Non-Sorptive Polymer-Lubricant Pairings

For PA46-pairings with almost non-spreading and non-swelling tendencies, an increasing surface hardness and stiction were found for increasing values of  $W_{\text{solving}}$  and  $W_{\text{spreading}}$ . In this case, the changes in the solving energy  $W_{\text{solving}}$  are related rather to local polymer-solvent interactions in the close vicinity of the polymer-solvent interface. Possible mechanisms are partially solved polymers at the surface, brush-like dangling chains, polymer transfer to the metal surface and/or an increased real contact. These are rather adhesive polymer-lubricant interactions compared with a reduction in cohesive forces by sorption. However, the understanding of these effects on a molecular level needs further research.

These non-sorptive pairings show a decrease in the wear rate for increasing values of  $W_{\text{solving}}$  and  $W_{\text{spreading}}$ , which is related to an increasing hardness and an increasing shear modulus. The changes in the mechanical properties are addressed to the thermal aging of the semicrystalline polymer matrix during storage. Chemical aging by degradation or post-crosslinking, post-crystallization or chemo-crystallization are possible mechanisms. The influence of different oils and especially polar pPG on the tribological properties is not yet understood. Different diffusivity and/or solubility of reaction products (or reactants) in the polymer matrix and the lubricants, respectively, are possible effects. For temperatures above the glass transition temperature of PA46,  $\mu_{\text{stiction}}$  is considerably lower as in the glassy state that is related to the solving character when the spreading character becomes irrelevant, such as for sorptive POM. This solving dependent behavior is explained by the higher molecular mobility in the amorphous phase above  $T_g$ .

## 5. Conclusions

Pairings of semicrystalline thermoplastic polymers with lubricants of different solubility within the polymer and different spreading tendencies were studied by oscillatory tribometry and standard gliding experiments to differentiate between tribological effects due to sorption and plasticization and those due to speeding.

Stiction, run-in wear and friction of polyoxymethylene (POM)- and polyamide (PA46)-lubricant pairings were studied under mild loaded mixed lubrication conditions. At room temperature, the amorphous phase of POM is in the rubber-like state, whereas it is in the glassy state for dry PA46. For the lubricants, a polar polyalkylene glycol (pPG), a non-polar polyalkylene glycole (nPG), an ester oil (EST), and a poly- $\alpha$ -olefin (PAO) solubility and spreading tendency were chosen. To elucidate the underlying molecular mechanisms, the tribological experiments were combined with material characterization. For this purpose, sorption measurements, dynamic mechanical analysis, and hardness measurements on unswollen and swollen specimens were performed. The samples are stored within the

solvents at 100 °C to reach equilibrium swelling/sorption prior to testing. To differentiate between sorption-induced effects and those due to thermal aging, unswollen samples were stored at the same temperature and for the same time in dry nitrogen and measured.

The main findings are:

- (1) Pairings of POM with Ester, nPG and pPG show a significant sorption of lubricants. The solving energy for the sorptive pairings is  $0 \text{ mN/m} < W_{\text{solving}} < 5 \text{ mN/m}$ . These pairings, show a significant dependence of run-in friction, stiction and wear on the equilibrium mass uptake of the lubricant. The sorption of lubricants leads to an increase in the real contact area due to a reduced mechanical modulus by the plasticization. Lubricant sorption and the related plasticization are found to depend on the solving energy  $W_{\text{solving}}$ . The tribological properties of the POM pairings are not sensitive to the spreading energy ( $W_{\text{spreading}}$ ), which is needed for separation of the metal and polymer interface by the lubricant. Only a small additional impact on the tribological properties due to thermal aging was found.
- (2) None of the PA46-lubricant pairings show a measurable mass uptake by sorption, and the tribological behavior is predominantly related to spreading and changes in hardness due to thermal aging. Near-surface effects due to the lubricants such as localized swelling, brush-like dangling chains, partial solution of polymer in the lubricant, mass transfer to the metal surface, etc., must be considered. These effects are also related to the interaction energies. For temperature above the glass temperature of PA46, the values of  $\mu_{\text{stiction}}$  are lower than those for the glassy state and decrease with the spreading energy. This can be explained by the significantly higher chain mobility above  $T_g$ .

In summary, the decrease in hardness and mechanical modulus due to sorption and plasticization was confirmed as the main factors for a decrease in wear rate with dominant abrasion behavior and mixed lubrication. Changes in chemical or semicrystalline structure during thermal treatment also influence hardness, which dominates abrasion and friction. In addition, specific interactions at the interface between the polymer and lubricant must be considered.

The influence of the roughness of the polymer, as well as the hard counterpart and the transfer of the polymer to the metal surface, needs to be investigated in the future. Furthermore, detailed investigations on the dependence of the real horizontal and vertical contact area on the plasticization, the temperature and the tribological parameters are required. The same applies to the viscoelastic and hysteretic mechanisms in the rubbery amorphous phase and the influences of the semicrystalline superstructure and the processing-related morphology gradients.

**Author Contributions:** Conceptualization, C.K.; investigation, C.K., O.P. and H.O.; writing, C.K., H.O. and I.A.; review and editing, I.A., B.S. and R.J. All authors have read and agreed to the published version of the manuscript.

**Funding:** The research leading to these results has received funding from the Federal Ministry for Economic Affairs and Climate of the Federal Republic of Germany under grant agreement no. 20375 N.

**Institutional Review Board Statement:** Not applicable.

**Informed Consent Statement:** Not applicable.

**Data Availability Statement:** Not applicable.

**Acknowledgments:** The authors are grateful for the financial support of AiF (Arbeitsgemeinschaft industrieller Forschungsvereinigungen) within the program for sponsorship by Industrial Joint Research (IGF) of the Federal Ministry for Economic Affairs and Climate Action (BMWK) based on an enactment of the German Parliament. The authors would also like to thank the Forschungsvereinigung Antriebstechnik e.V. and the Forschungsgesellschaft Kunststoffe e.V. for their appreciated technical support.

**Conflicts of Interest:** The authors declare no conflict of interest. The funding sponsors had no role in the design of the study; in the collection, analyses, or interpretation of data, in the writing of the manuscript, and in the decision to publish the results.

## References

1. Zhang, S.W. State-of-the-art of polymer tribology. *Tribol. Int.* **1998**, *31*, 49–60. [[CrossRef](#)]
2. Scherge, M.; Kramlich, J.; Böttcher, R.; Hoppe, T. Running-in due to material transfer of lubricated steel/PA46 (aliphatic polyamide) contacts. *Wear* **2013**, *301*, 758–762. [[CrossRef](#)]
3. Samyn, P.; Schoukens, G. Calculation and Significance of the Maximum Polymer Surface Temperature  $T^*$  in Reciprocating Cylinder-On-Plate Sliding. *Polym. Eng. Sci.* **2008**, *48*, 774–785. [[CrossRef](#)]
4. Koplín, C.; Abdel-Wahed, S.A.; Jaeger, R.; Scherge, M. The Transition from Static to Dynamic Boundary Friction of a Lubricated Spreading and a Non-Spreading Adhesive Contact by Macroscopic Oscillatory Tribometry. *Lubricants* **2019**, *7*, 6. [[CrossRef](#)]
5. Abdel-Wahed, S.A.; Koplín, C.; Jaeger, R.; Scherge, M. On the Transition from Static to Dynamic Boundary Friction of Lubricated PEEK for a Spreading Adhesive Contact by Macroscopic Oscillatory Tribometry. *Lubricants* **2017**, *5*, 21. [[CrossRef](#)]
6. Bormuth, A.; Bactavatchalou, R.; Rieder, A.; Kreiselmaier, R.; Zuleeg, J.; Groß, J.; Schmitz, J.; Spallek, R. Influence of Polymer-Lubricant Interaction on the Static Friction in Polymeric Tribo-Systems. In Proceedings of the International Conference on Trends in Agricultural Engineering, Prague, Czech Republic, 7–9 September 2016.
7. Briscoe, B. Wear of polymers: An essay on fundamental aspects. *Tribol. Int.* **1981**, *14*, 231–243. [[CrossRef](#)]
8. Schallamach, A. A theory of dynamic rubber friction. *Wear* **1963**, *6*, 375–382. [[CrossRef](#)]
9. Briscoe, B.J.; Sinha, S.K. Scratch Resistance and Localised Damage Characteristics of Polymer Surfaces—A Review. *Mater. Werkstofftech.* **2003**, *34*, 989–1002. [[CrossRef](#)]
10. Grosch, K.A. The Relation between the Friction and Visco-Elastic Properties of Rubber. *Proc. R. Soc. A Math. Phys. Eng. Sci.* **1963**, *274*, 21–39. [[CrossRef](#)]
11. Vorvolakos, K.; Chaudhury, M.K. The Effects of Molecular Weight and Temperature on the Kinetic Friction of Silicone Rubbers. *Langmuir* **2003**, *19*, 6778–6787. [[CrossRef](#)]
12. Chaudhury, M.K. Rate-Dependent Fracture at Adhesive Interface. *J. Phys. Chem. B* **1999**, *103*, 6562–6566. [[CrossRef](#)]
13. Singh, A.K.; Juvekar, V.A. Steady dynamic friction at elastomer–hard solid interface: A model based on population balance of bonds. *Soft Matter* **2011**, *7*, 10601. [[CrossRef](#)]
14. Sinha, N.; Singh, A.K.; Gupta, V.; Katiyar, J.K. Adhesive and normal stress-dependent dynamic friction of a gelatin hydrogel. *Proc. Inst. Mech. Eng. Part J J. Eng. Tribol.* **2021**, 135065012110446. [[CrossRef](#)]
15. Hentschke, R.; Plagge, J. Scaling theory of rubber sliding friction. *Sci. Rep.* **2021**, *11*, 18306. [[CrossRef](#)]
16. Kalin, M.; Polajnar, M. The Effect of Wetting and Surface Energy on the Friction and Slip in Oil-Lubricated Contacts. *Tribol. Lett.* **2013**, *52*, 185–194. [[CrossRef](#)]
17. Schertzer, M.; Iglesias, P. Meta-Analysis Comparing Wettability Parameters and the Effect of Wettability on Friction Coefficient in Lubrication. *Lubricants* **2018**, *6*, 70. [[CrossRef](#)]
18. CROW Polymer Properties. Barrier Properties of Polymers. Available online: <https://www.polymerdatabase.com/polymer%20physics/Permeability.html> (accessed on 27 March 2022).
19. Gooch, J.W. (Ed.) *Encyclopedic Dictionary of Polymers*; Springer: New York, NY, USA, 2011; ISBN 978-1-4419-6246-1.
20. Shipway, P.; Ngao, N. Microscale abrasive wear of polymeric materials. *Wear* **2003**, *255*, 742–750. [[CrossRef](#)]
21. Axén, N.; Jacobson, S. A model for the abrasive wear resistance of multiphase materials. *Wear* **1994**, *174*, 187–199. [[CrossRef](#)]
22. Grellmann, W. (Ed.) *Polymer Testing*, 3rd ed.; Hanser Publications: Cincinnati, OH, USA, 2022; ISBN 9781569908068.
23. Gebhardt, K.F. *Grundlagen der Physikalischen Chemie von Grenzflächen und Methoden zur Bestimmung Grenzflächenenergetischer Probleme*; IGB: Berlin, Germany, 1982.
24. Busscher, H.J.; van Pelt, A.W.J.; de Boer, P.; de Jong, H.P.; Arends, J. The effect of surface roughening of polymers on measured contact angles of liquids. *Colloids Surf.* **1984**, *9*, 319–331. [[CrossRef](#)]
25. Crank, J. *The Mathematics of Diffusion*; Oxford University Press: Oxford, UK, 1979; ISBN 0198534116.